

Oxidation Stages of Aluminium Nitride Thin Films Obtained by Plasma-enhanced Chemical Vapour Deposition (PECVD)

N. Azema,^a J. Durand,^{a*} R. Berjoan,^b C. Dupuy^b & L. Cot^a

^aLaboratoire de Physicochimie des Matériaux, URA 1312 du CNRS, 8 rue de l'Ecole Normale, 34053 Montpellier Cédex 1, France

^bInstitut de Science et de Génie des Matériaux et Procédés, BP 5, Odeillo, 66120 Font-Romeu, France

(Received 27 December 1990; revised version received 20 February 1991; accepted 6 March 1991)

Abstract

Oriented (100) aluminium nitride thin films grown on silicon wafers (100) and other substrates, were deposited at 330°C by the metal–organic PECVD process. The oxidation behaviour in air of these films was studied at temperatures from 500°C to 1300°C by X-ray diffraction, scanning electron microscopy and Auger electron spectroscopy. Two textural changes occur: granular and porous textures at 900°C and 1100°C, respectively. These correspond to the amorphous Al₂O₃ and the crystalline α -alumina formation. Infra-red absorption spectroscopy shows that the oxidation effectively starts at 600°C and reveals an oxynitride phase between the amorphous Al₂O₃ coating which is formed, and the AlN remaining.

Durch ein MOPECVD-Verfahren wurden bei 330°C auf Siliziumscheiben (100) und anderen Substraten orientierte dünne Schichten aus AlN (100) abgeschieden. Das Oxidationsverhalten dieser Schichten in Luft wurde im Temperaturbereich von 500°C bis 1300°C durch XRD, REM und AES untersucht. Zwei Veränderungen im Gefüge bilden sich: eine körnige Schicht bei 900°C und eine poröse bei 1100°C. Diese entsprechen dem amorphen Al₂O₃ und der α -Al₂O₃ Kristallmodifikation. Infrarotabsorptionsspektroskopische Untersuchungen konnten zeigen, daß die Oxidation bereits bei 600°C beginnt und daß zwischen dem sich bildenden amorphen Al₂O₃ Überzug und dem verbleibenden AlN eine Oxinitridphase vorliegt.

La croissance en couches minces de nitrure d'aluminium orienté (100), sur des plaquettes de silicium (100) et autres substrats, est obtenue à 330°C

par MOPECVD. Le comportement à l'oxydation à l'air de ces films est étudié par diffraction des rayons X, microscopie électronique à balayage et spectroscopie des électrons Auger, à des températures allant de 500°C à 1300°C. Deux changements de texture sont observés à 900°C et 1100°C, conduisant respectivement à des couches de type granuleux et poreux, correspondant à la formation d'alumine amorphe et d'alumine α cristallisée. La spectroscopie d'absorption infra-rouge met en évidence un début d'oxydation à 600°C ainsi que la présence d'un oxynitride d'aluminium entre la couche d'alumine amorphe et le nitrure d'aluminium non transformé.

1 Introduction

The wide field of aluminium nitride applications varies from dielectric to refractory compounds. It can be used as insulator in modern integrated circuits and is promising for optical uses because of its large energy band gap and masking ability.^{1,2} It is also an excellent substrate combining high thermal conductivity with high electrical resistivity for temperature-sensitive electronic components.^{3,4} It is applied in surface acoustic wave (SAW) techniques⁵ for its piezoelectric properties and high acoustic velocity. The passivation properties (for example in semiconductor devices for surface passivation or as diffusion masks⁶) and oxidation resistance⁷ have been the subject of recent papers. On the other hand, it appears that the humidity tolerance of AlN is a debatable point in the scientific community.

In recent years, the high-temperature protection of materials by ceramics, well known for their thermomechanic properties and chemical resistance, has attracted considerable interest. AlN may be a

* To whom correspondence should be addressed.

good candidate; nevertheless, few studies deal with the oxidation behaviour of AlN powder, bulk and thin films.^{8–11} A surface chemistry model has been written⁹ in which a gradual oxynitride layer (5–10 nm), formed on the surface, inhibits oxygen diffusion into the coating. Because of the increasing interest in this refractory material in thin layers and to provide a better understanding, it would be desirable to have data on its oxidation behaviour.

AlN films have been grown by various methods such as the chemical vapour deposition (CVD) process,^{12,13} reactive molecular beam epitaxy (MBE),¹⁴ ion beam sputtering,¹⁵ ion nitriding, etc. Recently, amorphous AlN thin films have been deposited at reasonably low temperatures (300–800°C), by metal-organic plasma enhanced chemical vapour deposition (MOPECVD).^{7,16} Hasegawa *et al.*¹⁶ investigated the possibility and conditions of deposition. The present authors use these conditions to determine certain deposition parameters such as radiofrequency (RF) power density, the substrate temperature, the choice of carrier and precursor gas, and the NH₃/TMA ratio. In this way, AlN thin films, with an oriented (100) structure, have been obtained on silicon (100) wafers. This original result differs from Hasegawa's previous papers, especially by the excitation frequency.

Thermal oxidation of these samples has been studied in air from 500°C to 1300°C by different methods of analysis. The film characteristics are investigated by scanning electron microscopy (SEM) and X-ray diffraction, and the elemental composition of the films is examined by Auger electron spectroscopy (AES), to determine the oxygen progress in the layer. On the other hand, infra-red absorption spectroscopy is a useful and non-destructive method to study the results of the heat treatment because of its sensitivity to changes in the external environment of the vibrating group.

2 Experimental

2.1 Deposition system

Figure 1 shows the schematic arrangement of the experimental tubular hot wall reactor. A parallel electrodes plasma CVD system is employed for this study. A 440 kHz generator is used to supply RF power which is capacitively coupled to the system. The silicon (100) substrate temperature is kept at 330°C. Trimethylaluminium (TMA), with nitrogen carrier gas (nitrogen, 5.0 purity of 99.999%), is introduced between the electrodes from a different gas line¹⁶ than the ammonia (ammonia, 4.5, purity of

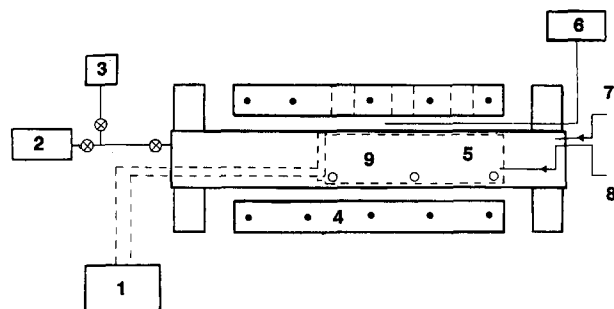


Fig. 1. Schematic representation of horizontal tube reactor used in this plasma CVD system: 1, RF power supply; 2, pump; 3, pressure control; 4, oven; 5, electrodes; 6, oven temperature control; 7, ammonia precursor; 8, TMA and nitrogen carrier gas; 9, samples.

99.995%). The background pressure of the system is around 0.9 Pa. The other synthesis conditions are a RF power density of 0.26 W cm⁻², a total pressure of 7 Pa, the aluminium precursor bubbler temperature around 55°C, and the NH₃/TMA ratio above 5.

AlN films are successfully obtained from this reactive system in a plasma atmosphere with a deposition rate about 1 μm/h, whereas it is impossible under thermodynamical equilibrium conditions at 330°C (in thermal CVD conditions, for example, 1200°C in Ref. 13).

2.2 Film characteristics

Scanning electron micrographs show uniform, dense AlN coatings with an excellent adherence and a very good step coverage on a wide variety of substrates (polished silicon wafers, graphite substrate or polycrystalline sintered silicon carbide), as can be seen in Figs 2 and 3. The surface shows a low defect density.

The refractive index, measured by ellipsometry, changes between 2.0 and 2.2 at the 5461 Å wavelength. These values are close to the reported values for crystalline AlN (2.17 for single-crystal AlN for a wavelength of 5890 Å¹⁷).

The X-ray diffraction pattern shows AlN coatings having a (100) preferential orientation (ASTM Data Card No. 25-1134), which is not influenced by the substrate: the same results are observed on silicon (111) or (100), silicon carbide and glass plates. On the other hand, the excitation frequency has an influence upon the material crystallinity: in a low-frequency field (440 kHz), AlN thin films are oriented along the *a*-axis, whereas in a high-frequency field (13.56 MHz) the material is amorphous.¹⁶

The surface ionic bombardment is an important parameter which influences adhesion, density, structure and stress¹⁸ of plasma deposits. The

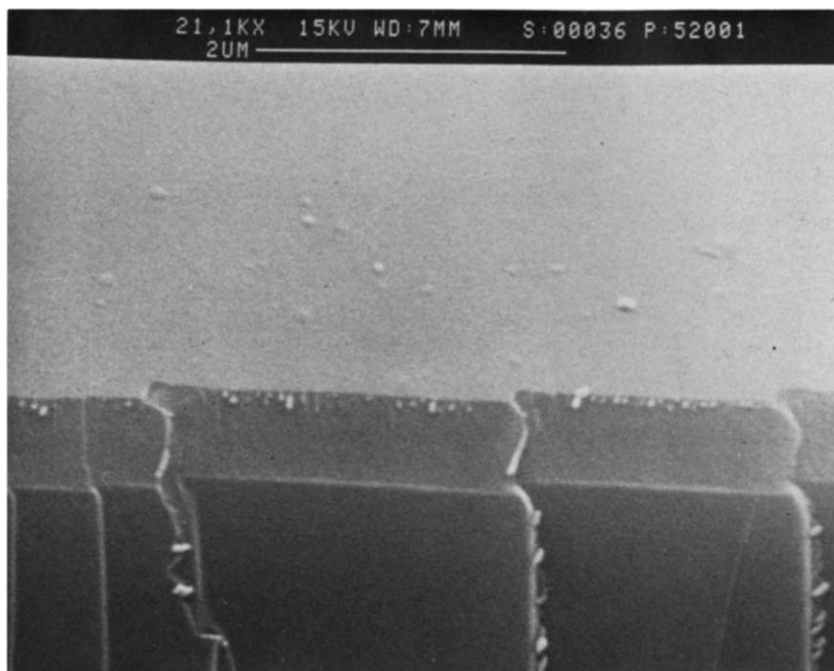


Fig. 2. AlN coating on silicon (100) substrate. The cracks are uninterrupted from substrate to the layer.

energetic particles inherent to the process cause intrinsic stresses in the coating which can be modulated principally by the excitation frequency.¹⁹ In this paper, intrinsic stresses are measured using the interference technique²⁰ with a thallium lamp. The measurement indicates tensile stresses in AlN (+268 MPa) obtained at a 440 kHz frequency. This value does not change up to 550°C.

Generally, in the plasma deposition process, the end products are realised with few impurities. This is just a function of the purity of the precursor gas, the gas delivery system and the reactor itself. Thereby,

the deposited films composition, measured by AES, reveals a percentage of carbon lower than 5%. No oxygen is detected (<1%), as can be seen in Fig. 4.

IR spectra of AlN deposited on silicon (100) wafers were taken using a Nicolet Fourier transform infra-red spectrometer (model 5ZDX). They show a broad, single strong peak at 670 cm^{-1} associated with the transverse optical vibration mode. Two other absorption-band areas have also been identified in Fig. 5: N—H (3205 cm^{-1}) and Al—H (2108 cm^{-1}), the hydrogen source in the film being the ammonia or TMA reactants.

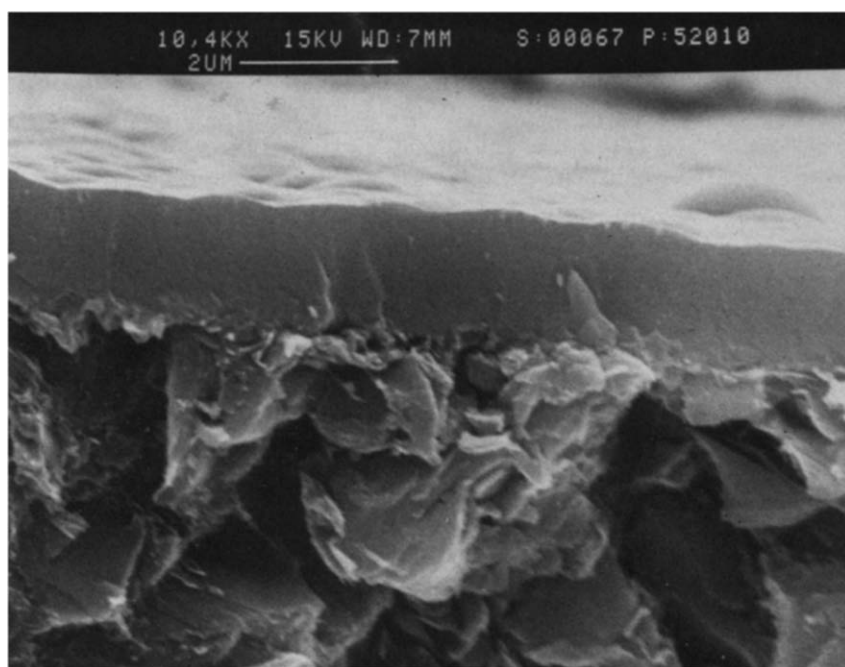


Fig. 3. Good step coverage of the AlN coating on graphite substrate.

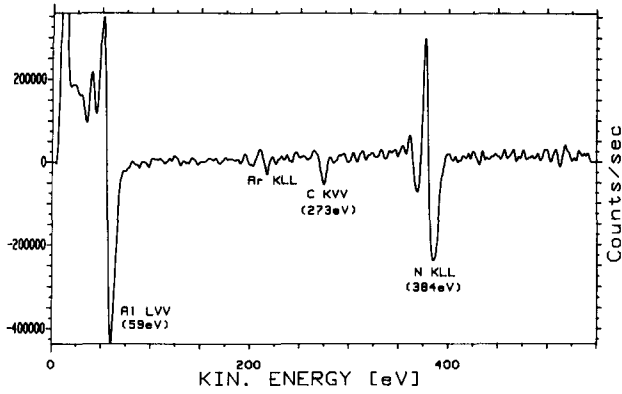


Fig. 4. dN/dE Auger electron energies spectra of AlN obtained by PECVD.

3 Oxidation of Aluminium Nitride Coatings

In this work, AlN thin films ($2\ \mu\text{m}$) deposited on silicon (100) were used. AlN samples in air are placed in the oven (the oven is kept open during treatments). Treatment temperatures are raised to the desired point at the rate of $150^\circ\text{C}/\text{h}$, kept constant for 45 min, and decreased to ambient temperature at the rate of $100^\circ\text{C}/\text{h}$.

3.1 X-Ray, SEM

The oxidation stages are first observed from X-ray diffraction data between 300°C and 1300°C . Up to 900°C only AlN (100) peaks are observed. The formation of an amorphous phase at 1000°C is indicated by the complete disappearance of all peaks. At 1100°C only $\alpha\text{-Al}_2\text{O}_3$ peaks are observed (Fig. 6).

Comparing this result to cross-section SEM micrographs, three different textures of coatings are observed (Figs 7–10). At the formation temperature

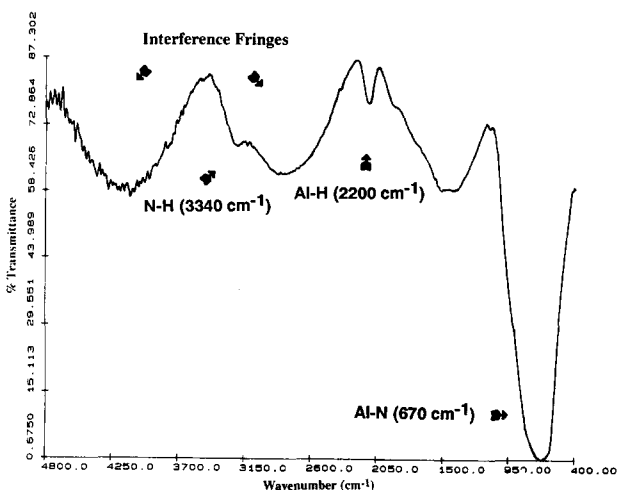


Fig. 5. Infra-red spectrum of AlN thin film deposited on silicon (100) wafers, with a thickness of $2\ \mu\text{m}$. (The silicon spectrum has been subtracted.)

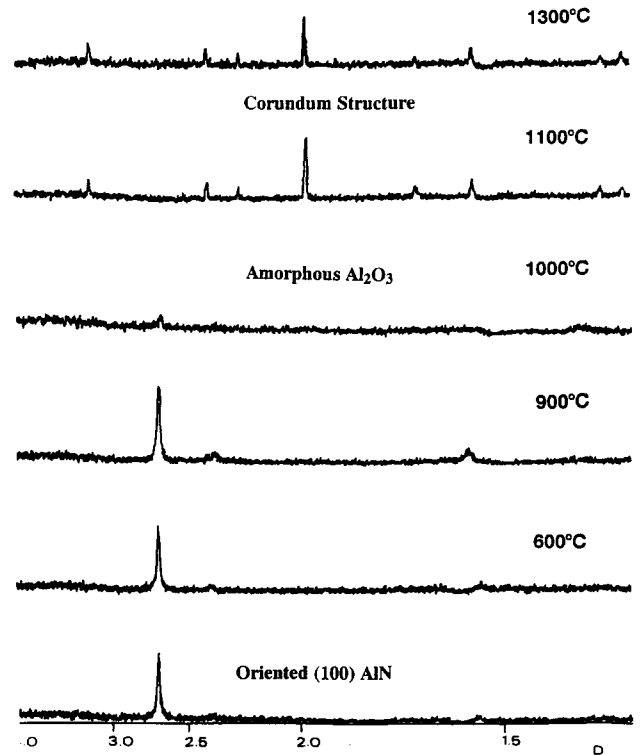


Fig. 6. Crystalline AlN transformation into a corundum structure shown by the X-ray diffraction pattern.

(330°C) and up to 800°C , the film is dense with a slightly columnar texture. During the heat treatments, two texture changes occur, resulting in granular and porous textures at 900°C and 1100°C , respectively. These correspond to the amorphous Al_2O_3 and the crystalline $\alpha\text{-alumina}$ formation known from sintered aluminium nitride,¹⁰ as shown by AES measurements (see Section 3.3).

3.2 Infra-red absorption spectroscopy

The oxidation of aluminium nitride samples starts at temperatures around 900°C . The refractive index is commonly measured by ellipsometry to determine the quality and the reproducibility of the plasma deposited films. For the thick samples ($>1\ \mu\text{m}$), interference fringes pattern of IR spectra are used to determine the thickness d , or the refractive index n , of the films at the normal incidence angle.²¹ The refractive index can be calculated by measuring the wavenumber difference between two minima or maxima of interference fringes according to the equation:

$$n = \Delta m / 2d \Delta v_{if}$$

where $\Delta m = m_i - m_f$ is the fringes number between the initial and final fringes, and $\Delta v_{if} = v_i - v_f$ is the wavenumber difference between the initial and final fringes. For the best estimation, Δv_{if} has been calculated from $4750\ \text{cm}^{-1}$ to $1150\ \text{cm}^{-1}$. In this

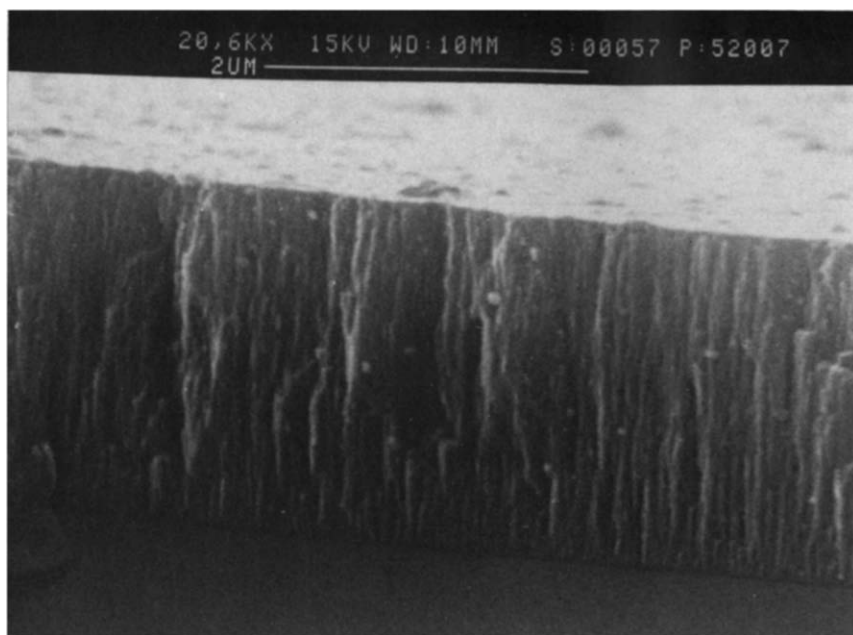


Fig. 7. AlN dense coating with a columnar texture synthesised at a temperature of 330°C. This texture is observed from 330°C to 800°C.

range of wavenumbers, only the N—H and Al—H weak band vibrations are observed; thus, the fringes are not disturbed.

In Fig. 11, high values of the refractive index are due to aluminium nitride,¹⁶ and the low values, to alumina.²² This diagram is in good agreement with X-ray and SEM data. The untreated film has a lower index values which may indicate impurities or a structural disorder.

The plasma-deposited materials often contain hydrogen as $\text{Si}_x\text{N}_y\text{:H}$,²³ $\text{Si}_{1-x}\text{C}_x\text{:H}$ ²⁴ or similar adducts. Precursor gas dissociation produces a greater amount of hydrogen which can be trapped in

the growing films. In the present work, hydrogen bonded to an aluminium atom is used as a probe of the presence of oxygen in thin films. It is known that the concept of localised group frequencies is modified by many other factors, and the results of these determine the precise position of the absorption band. Some of them are: changes of state, mass and coupling effects, strain and electrical effects. The last term can be considered as the most important in the present case (especially the inductive effects).

Figure 12(a) shows the oxygen influence on the Al—H bond vibration frequency. The model in Fig. 12(b) permits a good understanding of the pheno-

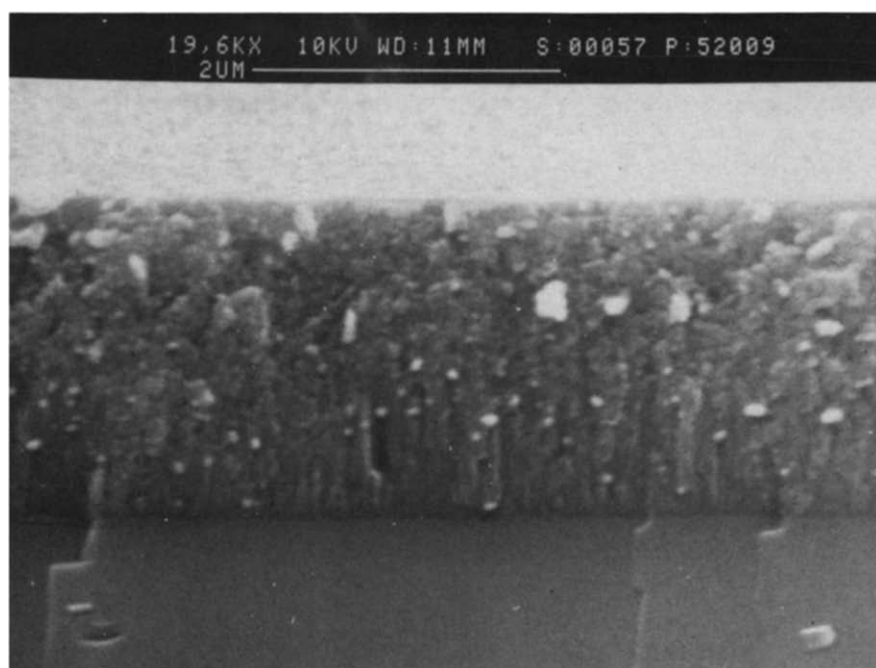


Fig. 8. Granular texture of amorphous Al_2O_3 and columnar texture of AlN, from 900°C to 1000°C.

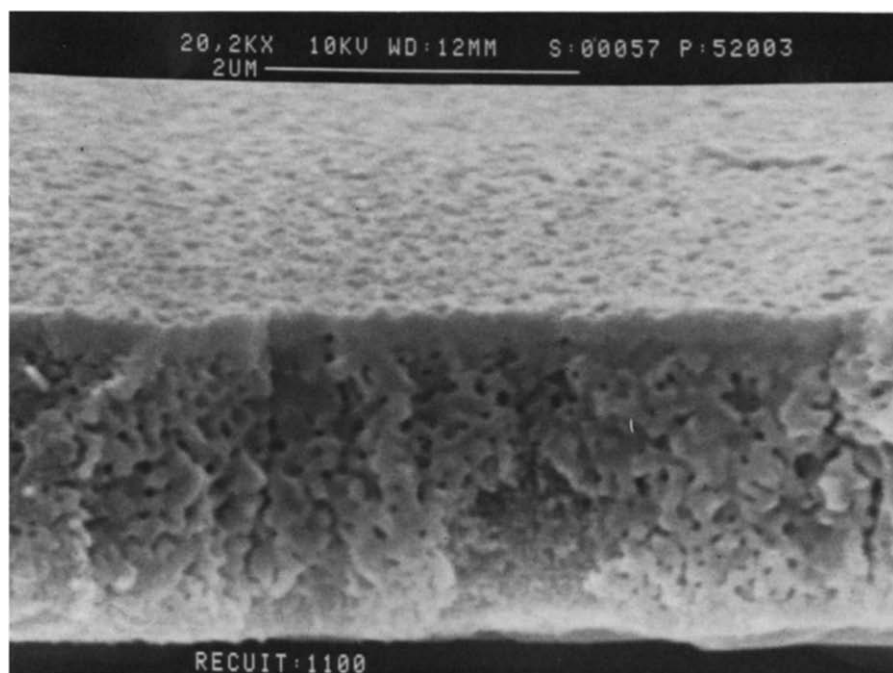


Fig. 9. Porous and granular textures of crystallised and amorphous alumina at 1100°C.

menon: the Al—H covalent bond has some degree of polar character. If a change is made in the electronegativity of the aluminium substituent (nitrogen substitution by oxygen), the polarity of the Al—H vibrating bond decreases; therefore the vibration frequency increases. Consequently, the Al—H stretching mode shift (2108 cm^{-1} to 2254 cm^{-1}) can be attributed to the increasing oxygen percentage. A limit exists at 600–900°C: two distinct Al—H bands can be observed on the IR spectra at temperatures just before the AlN transformation to $\alpha\text{-Al}_2\text{O}_3$. It may indicate two different

phases: the first band corresponds to the non-transformed AlN and the other to an oxynitride phase.

3.3 Auger electron spectroscopy

The sample Auger electrons are analysed by a Riber MAC-2 Auger spectrometer. The AES measurements are taken at different ionic sputtering times for every sample; parameters such as the primary electron energy of the beam, the gun electron emission current and the energy ionic sputtering are kept constant. The sputtering rate is about 30 to

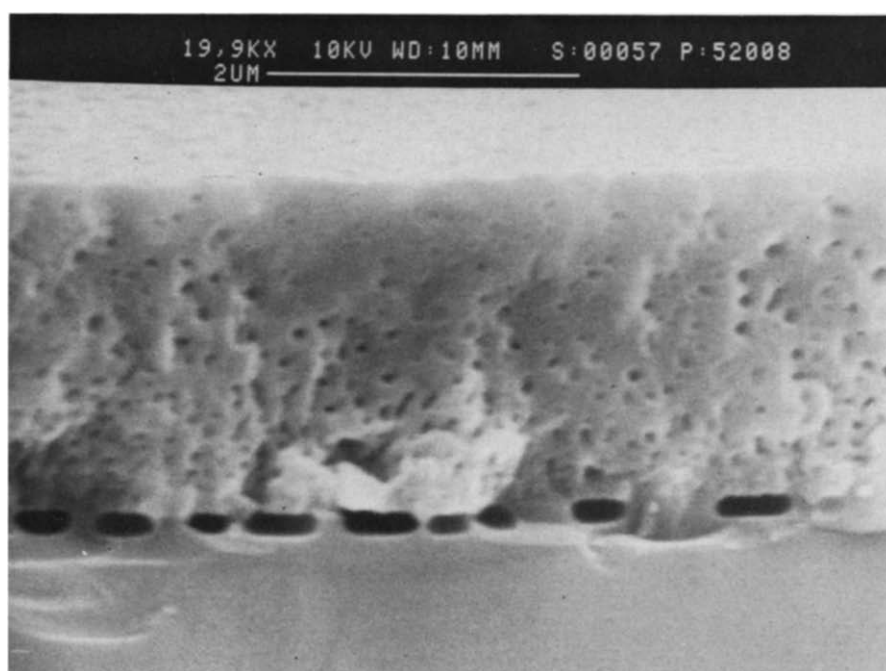


Fig. 10. Porous texture of α -alumina from 1200°C to 1300°C.

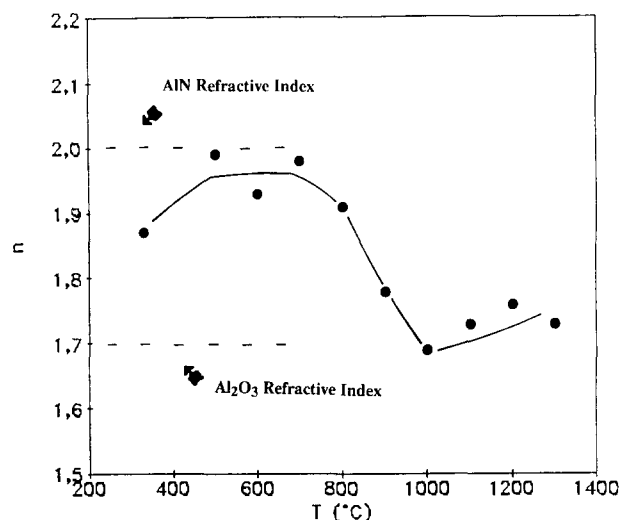


Fig. 11. Refractive index variation according to temperature treatments. The refractive index is obtained from the interference fringes pattern of IR spectra.

50 Å/min. The authors were interested in the oxygen concentration profiles in the AlN coating annealings. They have been obtained from the product of the kinetic energy by the number of collected electrons having this energy $E.N(E)$ Auger spectra, scanned in the range between 50 and 520 eV. The intensity of the KLL Auger transition for the oxygen atom (OKLL) at 510 eV has been determined by measuring heights of the peak with respect to the level of the background.²⁵

The results of the peak to background ratio (P/B) variation versus sputtering time shown in Fig. 13 are in good agreement with the previous studies. The initial stage of oxidation is the oxide formation on the surface (100–200 Å). The 300, 600 and 700°C curves show a decrease to negligible values of the oxygen. The P/B are significant of a gradual AlO_xN_y intermediate area rather than alumina, between the native oxide layer and the nitride remaining. This oxynitride layer has a thickness which is not greater than 1000 Å. Up to 900°C the P/B values are constant and correspond to alumina. In this case, the sputtering conditions have not permitted the hollowing out of the coating to reveal the aluminium oxynitride and the nitride observed at 900°C by IR. Beyond 900°C a thick alumina coating is formed.

4 Conclusion

For the first time, aluminium nitride thin films obtained by the MOPECVD process have a (100) crystalline orientation. The coatings are dense, adherent and show a good step coverage and few impurity incorporations. Their oxidation behaviour

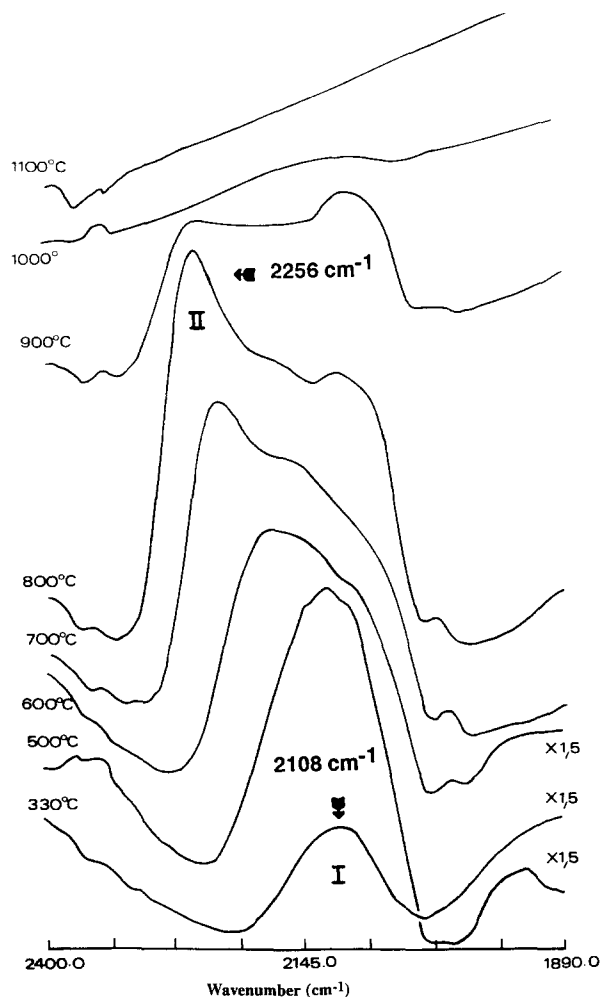


Fig. 12. (a) Effect of aluminium environment on Al—H bond vibration frequency.

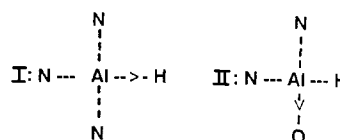


Fig. 12. (b) Model showing the nitrogen substitution by oxygen. The polar character of the Al—H vibration bond decreases and also the vibration frequency increases.

is identical to AlN powders. X-Ray diffraction, SEM and AES show two transformations at 900°C and 1100°C which correspond respectively to the AlN transformation into amorphous Al_2O_3 , and the amorphous phase into the corundum structure. Nevertheless, by the study of the Al—H vibrating band shift, IR spectroscopy reveals that the oxidation of AlN thin films starts at 600°C. The formation of an oxynitride layer between the aluminium nitride and alumina is observed. The alumina coating is amorphous at 1000°C and crystallises at 1100°C in $\alpha-Al_2O_3$.

This work is just a step towards coatings for anti-oxidation protection at high temperatures. The use

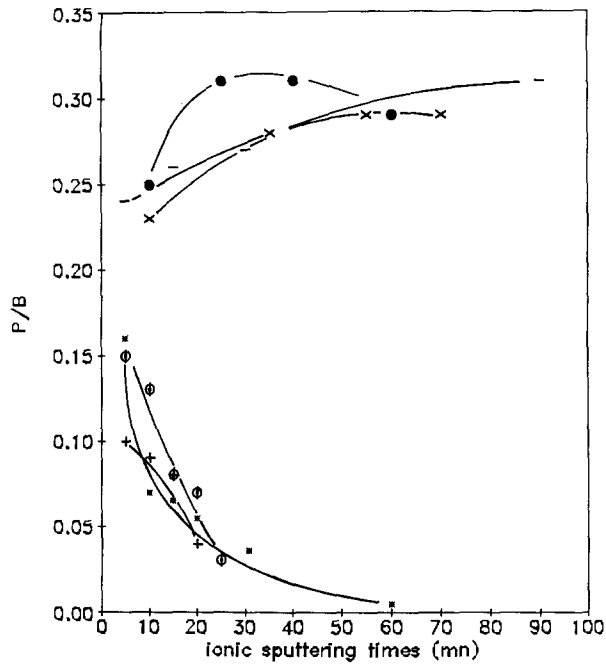


Fig. 13. Oxygen concentration–depth profile at different temperature treatments obtained from the AES spectra. Φ , 300°C; +, 600°C; *, 700°C; ●, 900°C; ×, 1000°C; −, 1100°C.

of multilayers or gradual layers, which include AlN coating(s), might be a better way to stop oxygen diffusion.

References

1. Yim, W. M., Stofko, E. J., Zanzucchi, P. J., Pankove, J. I., Ettenberg, M. & Gilbert, S. L., Epitaxially grown AlN and its optical band gap. *J. Appl. Phys.*, **44** (1973) 292–6.
2. Bauer, J., Biste, L. & Bolze, D., Optical properties of aluminium nitride prepared by chemical and plasma-chemical vapour deposition. *Phys. Stat. Sol. (a)*, **39** (1977) 173–81.
3. Kurokawa, Y., Utsumi, K., Takamisawa, H., Kamata, T. & Noguchi, S., AlN substrates with high thermal conductivity. *IEEE Transactions on Components, Hybrids and Manufacturing Technology*, **CHMT-8** (1985) 247–52.
4. Feil, M., Experience with AlN substrate. *Hybrid Circuits*, **18** (1989) 29–34.
5. Dobrynin, A. V., Naida, G. A. & Novoselov, V. A., Acoustoelectric parameters of aluminium nitride epitaxial layers. *Phys. Stat. Sol. (a)*, **104** (1987) K47–K51.
6. Lewis, D. W., Properties of aluminum nitride derived from $\text{AlCl}_3 \cdot \text{NH}_3$. *J. Electrochem. Soc.*, **117** (1970) 978–82.
7. Itoh, H., Kato, M. & Sugiyama, K., Plasma-enhanced chemical vapour deposition of AlN coatings on graphite substrates. *Thin Solid Films*, **146** (1987) 255–64.
8. Abid, A., Bensalem, R. & Sealy, B. J., The thermal stability of AlN. *J. Mat. Sci.*, **21** (1986) 1301–4.
9. Hatwar, T. K. & Pian, T. R., Surface studies of aluminium nitride thin films. *Mat. Res. Soc. Symp. Proc.*, **121** (1988) 557–60.
10. Lavrenko, V. A. & Alexeev, A. F., Oxidation of sintered aluminium nitride. *Ceramics International*, **9** (1983) 80–2.
11. Katnani, A. D. & Papatthomas, K. I., Kinetics and initial stages of oxidation of aluminum nitride: thermogravimetric analysis and X-ray photoelectron spectroscopy study. *J. Vac. Sci. Technol.*, **A5** (1987) 1335–40.
12. Pauleau, Y., Bouteville, A., Hantzpergue, J. J. & Remy, J. C., Composition, kinetics, and mechanism of growth of chemical vapor-deposited aluminum nitride films. *J. Electrochem. Soc.*, **129** (1982) 1045–52.
13. Morita, M., Uesugi, N., Isogai, S., Tsubouchi, K. & Mikoshiba, N., Epitaxial growth of aluminum nitride on sapphire using metalorganic chemical vapor deposition. *Japan. J. Appl. Phys.*, **20** (1980) 17–23.
14. Yoshida, S., Misawa, S., Fujii, Y., Takada, S., Hayakawa, H., Gonda, S. & Itoh, A., Reactive molecular beam epitaxy of aluminium nitride. *J. Vac. Sci. Technol.*, **16** (1979) 990–3.
15. Dehuang, W., Sputtered AlN films for semiconductor lasers. *Thin Solid Films*, **187** (1990) 127–32.
16. Hasegawa, F., Takahashi, T., Kubo, K. & Nannichi, Y., Plasma CVD of amorphous AlN from metalorganic Al source and properties of the deposited films. *Japan. J. Appl. Phys.*, **26** (1987) 1555–60.
17. Pastrnak, J. & Roskovicova, L., Refraction index measurements on AlN single crystals. *Phys. Stat. Sol. (a)*, **14** (1966) K5–K8.
18. Catherine, Y., Croissance de couches minces sous flux d'ions. In *Journées d'études: Interaction plasmas froids matériaux*. Oléron (1987). Editeur Scientifique, GRECO 57—Editions de physique, Paris, 319–39.
19. Hess, D. W., Plasma-enhanced CVD: Oxides, nitrides, transition metals, and transition metal silicides. *J. Vac. Sci. Technol.*, **A2** (1984) 244–52.
20. Finegan, J. D. & Hoffman, R. W., Stress and stress anisotropy in iron films. In *Trans. 8th Natl Vacuum Symp.* Pergamon Press, New York, 1961, pp. 935–42.
21. Harrick, N. J., Determination of refractive index and film thickness from interference fringes. *Applied Optics*, **10** (1971) 2344–9.
22. Schemmel, T. D., Cunningham, R. L. & Randhawa, H., Process for high rate deposition of Al_2O_3 . *Thin Solid Films*, **181** (1989) 597–601.
23. Wang, S. L., Cheng, R. G., Qi, M. W. & Cai, P. X., IR and H evolution spectrum of $\alpha\text{-SiN}_x\text{:H}$ with different nitrogen content. *J. Non-Cryst. Sol.*, **97–98** (1987) 1039–42.
24. Basa, D. K. & Smith, F. W., Annealing and crystallization processes in a hydrogenated amorphous Si–C alloy film. *Thin Solid Films*, **192** (1990) 121–33.
25. Langeron, J. P., Minel, L., Vignes, J. L., Bouquet, S., Pellerin, F., Lorang, G., Ailloud, P. & Le Héricy, J., The use of peak to background ratio in quantitative Auger analysis. *Solid State Communication*, **49** (1984) 405–7.